Available online at www.sciencedirect.com
ScienceDirect
Global and Planetary Change 54 (2006) 183–201
GLOBAL AND PLANETARY CHANGE
www.elsevier.com/locate/gloplacha

Meteorological impact assessment of possible large scale irrigation in Southwest Saudi Arabia

H.W. Ter Maat [a,*], R.W.A. Hutjes [a], R. Ohba [b], H. Ueda [c], B. Bisselink [a], T. Bauer [a]

[a] *Alterra, Wageningen, The Netherlands*
[b] *Mitsubishi Heavy Industries, Nagasaki, Japan*
[c] *Acid Deposition and Oxidant Research Center, Niigata, Japan*

Received 22 August 2005; received in revised form 21 December 2005; accepted 19 January 2006
Available online 28 July 2006

Abstract

On continental to regional scales feedbacks between landuse and landcover change and climate have been widely documented over the past 10–15 years. In the present study we explore the possibility that also vegetation changes over much smaller areas may affect local precipitation regimes. Large scale ($\sim 10^5$ ha) irrigated plantations in semi-arid environments under particular conditions may affect local circulations and induce additional rainfall. Capturing this rainfall 'surplus' could then reduce the need for external irrigation sources and eventually lead to self-sustained water cycling.

This concept is studied in the coastal plains in South West Saudi Arabia where the mountains of the Asir region exhibit the highest rainfall of the peninsula due to orographic lifting and condensation of moisture imported with the Indian Ocean monsoon and with disturbances from the Mediterranean Sea.

We use a regional atmospheric modeling system (RAMS) forced by ECMWF analysis data to resolve the effect of complex surface conditions in high resolution (Δx=4 km). After validation, these simulations are analysed with a focus on the role of local processes (sea breezes, orographic lifting and the formation of fog in the coastal mountains) in generating rainfall, and on how these will be affected by large scale irrigated plantations in the coastal desert.

The validation showed that the model simulates the regional and local weather reasonably well. The simulations exhibit a slightly larger diurnal temperature range than those captured by the observations, but seem to capture daily sea-breeze phenomena well. Monthly rainfall is well reproduced at coarse resolutions, but appears more localized at high resolutions. The hypothetical irrigated plantation ($3.25\ 10^5$ ha) has significant effects on atmospheric moisture, but due to weakened sea breezes this leads to limited increases of rainfall. In terms of recycling of irrigation gifts the rainfall enhancement in this particular setting is rather insignificant.
© 2006 Elsevier B.V. All rights reserved.

Keywords: land-use change; irrigation; regional weather; mesoscale modeling; semi-arid environment; Saudi Arabia

1. Introduction

Feedbacks between landuse and landcover change and weather and climate have been widely documented over the past 10–15 years, on both global and continental and regional scales (e.g. Kabat et al., 2004; Pielke et al., 2002). A substantial subset of this literature

* Corresponding author. Alterra, PO Box 47, 6700 AA Wageningen, The Netherlands. Tel.: +31 317 474278; fax: +31 317 419000.
E-mail address: herbert.termaat@wur.nl (H.W. Ter Maat).

0921-8181/$ - see front matter © 2006 Elsevier B.V. All rights reserved.
doi:10.1016/j.gloplacha.2006.01.018

focuses on landuse climate interactions in semi-arid regions often analyzing the relative role humans may have played in issues of desertification (e.g. Reynolds and Stafford-Smith, 2002). One of the more intensely studied systems is that of western Africa, where after the landmark paper of Charney (1975) a large number of (modelling) studies revealed linkages between (human induced) vegetation degradation and subsequent rainfall decreases in the Sahel (for a review see Xue et al., 2004). Vice versa the very occurrence of vegetation may have contributed to a wetter climate that occurred in prehistoric times in that region (Claussen et al., 1999), in turn starting-off studies into the potential regreening of the Sahara (Claussen et al., 2003). More generalized, Koster et al. (2004) explored the sensitivity of regional climates around the world to land surface interactions and found profound feedback effect in areas in the Mid-US, Africa and India.

The basic mechanism is that a land cover or landuse change modifies the radiation balance and the subsequent partitioning of available energy over sensible or latent heat fluxes. These are first order effects and their relative importance may vary spatially and in time. Differences in latent and sensible heat input lead to altered heat and moisture content of the atmospheric boundary layer (ABL). ABL temperature and humidity feed back to the surface through stomatal behaviour of plants, creating a first potential loop. ABL temperature and humidity affect convective heating, total diabatic heating, subsidence, monsoon-flow strength and moisture convergence. These processes all affect cloud formation and as clouds strongly affect radiation a second potential feedback loop comes into play. If altered clouds also affect precipitation, additional feedback loops are activated through soil moisture stores, vegetation growth and phenology and eventually ecosystem changes/displacements. Each of these potential feedback loops (in the order discussed) acts on increasingly longer timescales.

Similar effects have been reported on smaller regional scales as a consequence of irrigation for agricultural purposes, and for a long time already the notion is prevalent that large scale irrigation may affect rainfall over or downwind of the irrigated area (Schickedanz and Ackermann, 1977; Ben-Gai et al., 1993). In broad lines the relationships between weather or climate and irrigation are similar as those outlined above but the generally smaller spatial scales bring different mechanisms into play. The net effect is the sum of several opposing mechanisms. Obviously irrigated agriculture, through enhanced evaporation, will increase the vapor content of the (lower) atmosphere. However, at the same time the big thermal contrast between the cool, wet irrigated area and its hot, dry surroundings may create its own local circulation leading to downward motions over the area, thus decreasing the likelihood of precipitation. Whether this happens depends on the size of landscape patchiness that is needed before the boundary-layer structure is significantly affected and a mesoscale circulation produced, an issue explored by many authors (Avissar and Schmidt, 1998). Conversely, in a coastal setting the cooling over the irrigated area may hinder the development of true sea breezes circulation preventing imported marine moisture to precipitate (Lohar and Pal, 1995). Also, combined cooling and wetting of the atmosphere may increase low level instability, thereby triggering storms (Moore and Rojstaczer, 2002). In these cases the main effect does not come from additional atmospheric moisture supplied by irrigation but rather through modification of local to regional dynamics that convert advected moisture into precipitation. For the same reason the rainfall enhancement may not occur over the irrigated area but some distance downwind, in the study by van der Molen (2002) up to 90 km downwind.

The extent to which irrigation produces additional rainfall differs case by case. Moore and Rojstaczer (2002) found a 6–18% increase on a total of ~200 mm in summer rainfall in the Texas High plains. Ben-Gai et al. (1993) found a 100–300% increase in October rainfall in Southwest Israel though absolute numbers were small 5–15 mm). Miglietta (personal communication) reported a 90% (equivalent to 16 mm) increase in July–August rainfall for the Capitanata irrigation scheme in central Italy.

In the context of irrigation induced precipitation enhancement it is useful to invoke the concept of a recycling ratio: the fraction of evaporated water that is converted into precipitation. If this recycled water falls within the irrigated area or downwind but still within the catchment used to supply irrigation water it may reduce the need for irrigation water from other, more environmentally detrimental sources like deep wells or desalinisation plants. Recycling, when sufficiently strong, may open up the possibility, after initial irrigation of a more self-sustained agriculture. Sud et al. (2001) found that the recycling ratio was more a function of background circulation than of local evaporation and remarkably robust for a large range of vegetation covers, soil types, and initial soil moistures. They found recycling ratios of 25–50% in wet conditions decreasing to <1–7% in dry synoptic conditions. In the study by Moore and Rojstaczer (2002) recycling amounted to about 10%.

In the present study we also explore the idea that large scale (~10^5 ha) irrigated plantations in semi-arid environments under particular conditions can modulate a patterning of the rainfall. As a case study area we focus on

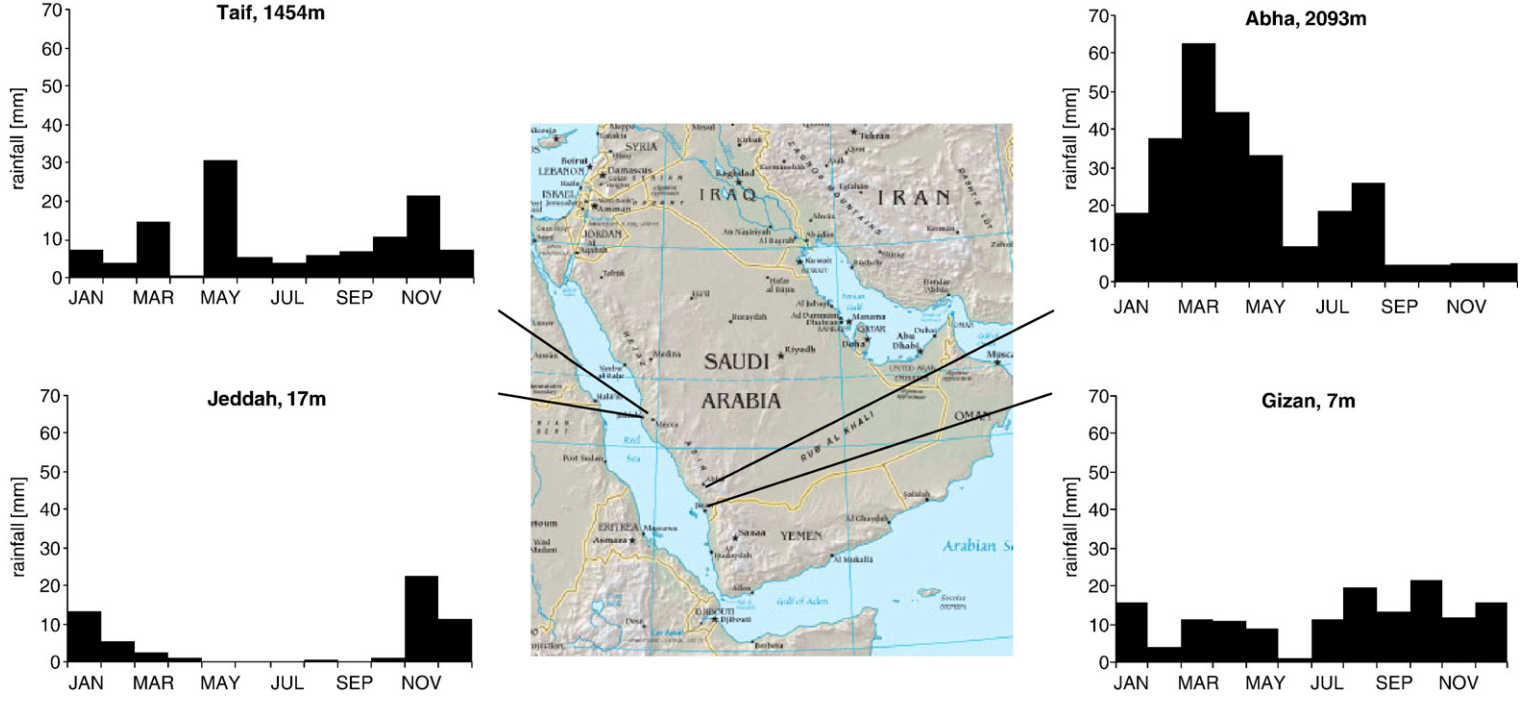

Fig. 1. Averaged rainfall observations for stations in Southwest Saudi Arabia. Taif data are averaged over 1961–1990 and the other station data over 1978–2001.

Table 1
RAMS4.4 configuration

	High resolution grid	Coarse resolution grid
d*x*, d*y*	4 km (125 × 125 gridpoints)	80 km (60 × 62 gridpoints)
d*t*	10 s	90 s
Dz	100 stretching to 750 m (37 levels)	
Topography	DEM USGS (~1 km resolution)	
Radiation	Chen and Cotton (1983)	
Land surface model	LEAF-2 (Walko et al., 2000)	
Diffusion	Mellor/Yamada (1982)	
Nudging time scale	Lateral 1800 s	Lateral 1800 s, centre 7200 s
Convection	Full microphysics package (Flatau et al., 1989)	Modified Kuo convection scheme (Tremback, 1990)

Southwest Saudi Arabia where plans are in exploratory stages of development to construct large scale irrigation works in its coastal plains, based on freshwater produced from sea water through sustainable de-salinisation techniques using solar or biomass energy. These plains are confined between the Red Sea in the west providing a lot of atmospheric moisture input, and the high Asir mountain range to the east which orographically force air to lift, potentially to condensation levels. These mountain ranges exhibit the highest rainfall of the Arabian Peninsula and sustain quite some traditional rainfed agriculture. In Koster et al. (2004; his Fig. 1) the southwest part of Arabia appears to have some potential strength in land–atmosphere coupling, even though not as profound as in the Mid-US, Africa and India.

The RAMS model (Regional Atmospheric Modelling System) has been implemented for the region and has been used to explore the impact of a hypothetical large scale irrigated plantation on the meteorology, in particular rainfall, of the region. The source of irrigation water and its application and distribution technicalities or societal impacts are of no concern in the present analysis, but are under study elsewhere. We will simply assume enough irrigation water will somehow be available to sustain more vegetation than is presently growing in a particular area. First we will validate the model using actual (little) vegetation and (low) soil moisture conditions in a control run. Next we will present results from runs with a large area with denser vegetation and higher soil moisture levels, followed by a discussion of these results, plausible causal mechanisms and broader implications. Finally, we will discuss to which extend capturing this rainfall 'surplus' could then reduce the need for external irrigation sources and eventually lead to self-sustained water cycling.

2. Description of regional climate

Saudi Arabia is one of the hottest and driest countries in the world with precipitation ranging from 50 to 80 mm for most of the country. Our study area, the southwestern part of the country including the Asir Mountain range, records mean annual precipitation rates of 250 mm which is the country's highest rainfall. This is due to orographic lifting and condensation of moisture imported with the Indian Ocean monsoon and with disturbances originating from the Mediterranean Sea (Chakraborty et al., 2006). From this mountain range, with elevations up to 3000 m above sea level, the dry interior plateau slopes gently to the Arabian Gulf east of the country. Between this mountain range and the Red Sea to the west lies a narrow coastal plain with a width of around 100 km. As a result of the spatial distribution of rainfall, the agriculture in the mountains is mostly rainfed in contrast with the coastal plains where irrigation water is extracted from the ground.

The distribution of rainfall over the year and for different stations in Southwest Arabia is given in Fig. 1. Two rainfall peaks can be distinguished for Abha and Gizan (cities in the mountains and coastal plain respectively) from March till May and in late summer. The first peak is a result of an unstable transition period from the Mediterranean to the monsoonal effect (Bazuhair et al., 1997) and the second peak when the monsoon transports water vapor in Southwest Arabia. To the north (Taif and Jeddah), this monsoonal circulation is absent and the Mediterranean influence prevails with a period of heavy rainstorms between November and February. The influence of the monsoonal system is limited because of the strong continental air mass, which prevails over the Arabian Peninsula from June to September. Not shown here is the temporal distribution of temperature over the year, which is strongly seasonal.

3. Description of experiment

To study the regional circulations and the meteorological impact of large scale irrigation combined with a landuse change, for the southwestern part of Saudi Arabia, the Regional Atmospheric Modelling System (RAMS version 4.4; Cotton et al. (2003)). The model is 3D, non-hydrostatic based on fundamental equations of fluid dynamics and includes a terrain following vertical coordinate system. One of the advantages of RAMS is the possibility to perform simulations on high resolution meshes to model small-scale atmospheric systems.

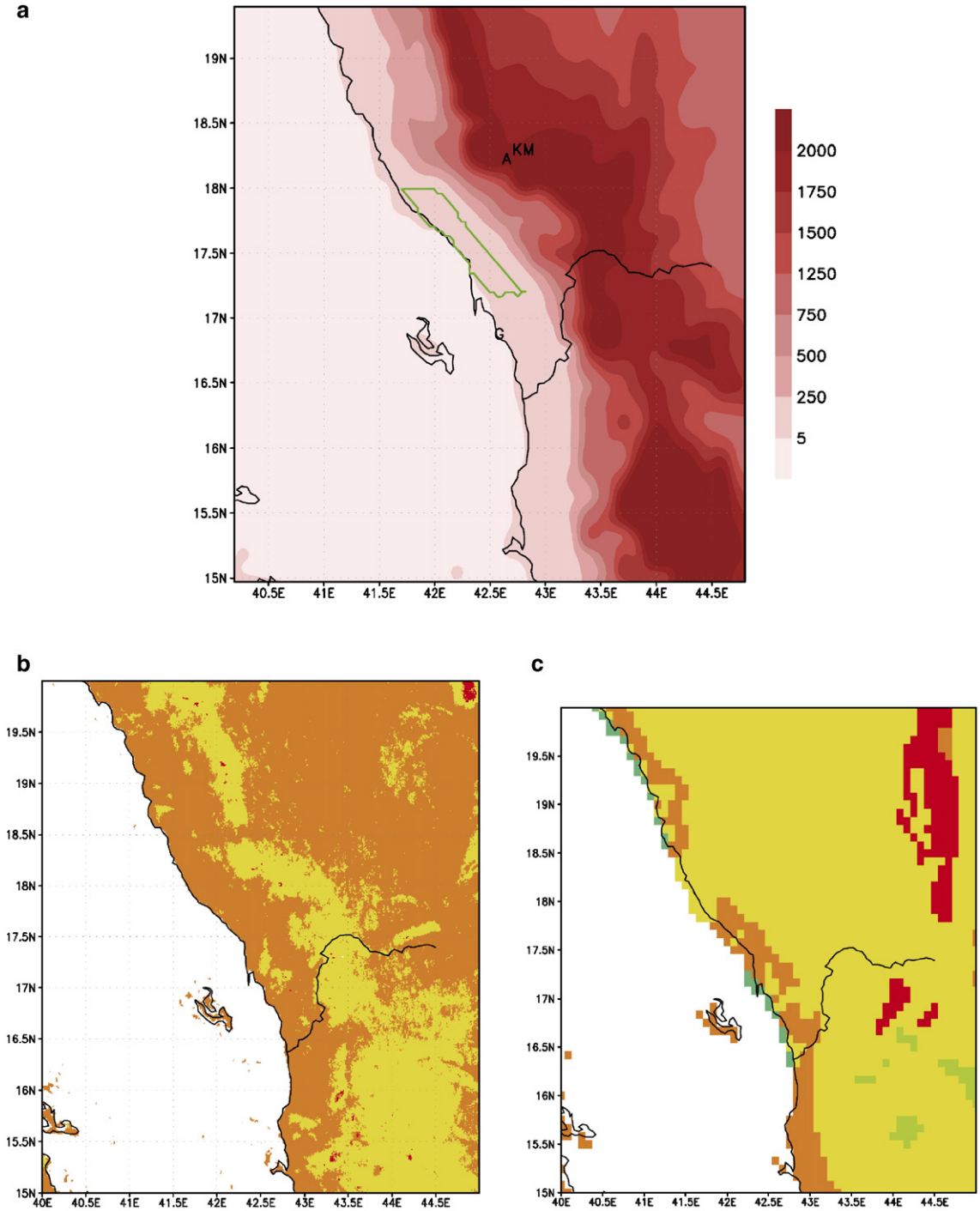

Fig. 2. Study area Saudi Arabia: a) Topography (m) and location of the meteorological stations (A — Abha, KM — Khamis Mushayt, G — Gizan). The green line show the outline of the hypothetical irrigated plantation implemented in the 'green' simulation. b) Land cover classification (yellow: semi-desert, orange: desert, red: other landuse classes, mainly urban areas) c) Soil texture classification (yellow: loam, orange: silt loam, red: loamy sand, green: sandy clay loam). (For interpretation of the references to colour in this figure legend, the reader is referred to the web version of this article.)

In this study RAMS has been used in two configurations: a nested and a single grid configuration. The nested configuration had a large domain covering the Arabian Peninsula and part of the horn of Africa with two smaller domains (16 km and 4 km) zooming in on an area centred on Abha and Gizan. The smallest nested domain, as well as the stand alone domain had a horizontal grid spacing of 4 km covering Southwest Arabia, West Yemen and part of the Red Sea. Both simulations are executed for the period from 21 February until 15 May 2000 covering the wettest period of the year (Fig. 1). Table 1 shows the various options/parametrizations which are used in RAMS for this study. Fig. 2a shows the area which is used in the high resolution simulations and this figure also shows the details of the topography. The mountain range can clearly be distinguished together with the narrow coastal area between the mountains and the Red Sea.

RAMS is forced by analysis data from the European Centre for Medium-Range Weather Forecasts (ECMWF) global model. The grid spacing of the forcing data is 0.5° by 0.5° and available every 6 h. Monthly sea surface temperatures have been extracted from the Met Office Hadley Centre's sea ice and sea surface temperature (SST) data set, HadISST1 (Rayner et al., 2003).

The following databases have been used to prescribe the land cover and the soil texture in the area (Fig. 2b, c). Landuse classes have been extracted from the USGS database (Loveland et al., 2000) with a resolution of around 1 km which is standard within the RAMS framework. Soil properties (not standard in RAMS) were derived from the IGBP-DIS Soil Properties database (Global Soil Data Task Group, 2000) which has a resolution of approximately 10 km.

To validate the results of the control simulation of RAMS surface observations and satellite products are used. Validating a regional model in an area where data availability at the surface is scarce is not trivial, and therefore satellite products are necessary in validating model output. The surface observations are extracted from the ECMWF observational archive at the main synoptic hours (0:00, 6:00, 12:00 and 18:00 UTC). The variables of interest from this database are dry bulb temperature (K), windspeed (m s^{-1}) and wind direction (deg). Table 2 shows the surface stations used in the validation. The satellite data used in this paper are extracted from the Tropical Rainfall Measuring Mission (TRMM) satellite, which was launched 27 November 1997 (Huffman et al., 1995). This satellite estimates among others rainfall rates and accumulated precipitation. We used the 3B43 data product, a merged product combining satellite derived estimates with ground observations. It is available (and used here) in two spatial resolutions, on a 0.25° and a 1° resolution for the area bounded in the north and south by the 50-degree latitude, in both cases on a monthly basis.

Table 2
Weather stations used for validation

Station	WMO code	Latitude (deg)	Longitude (deg)	Elevation (m)
Abha	41112	18.23N	42.65E	2093
Khamis Mushait	41114	18.3N	42.8E	2056
Gizan	41140	16.88N	42.58E	7

The stations are identified by WMO code.

After validation of our control simulations, this paper will focus on meteorological effects caused by large scale irrigation in combination with landuse change. The area designed for this landuse change is indicated as a green outline in Fig. 1. With regards to the location of the plantation, it is hypothesized that more moisture will be available above the irrigated plantation and that, subsequently, this moisture will be transported by the southwestern wind inland (sea breeze) and that, subsequently, orographic lifting might generate more rainfall in the Asir Mountains downwind of the plantation. The landuse of the irrigated plantation has been changed from desert into shrubland over an area of approximately 36 km by 90 km. This change leads to a change in albedo from 0.3 to 0.1 and in roughness length from 0.05 m to 0.14 m. These values are in LEAF defined from the BATS vegetation scheme (Dickinson et al., 1986). The size of the plantation is equivalent to 9 × 22 gridpoints in the high resolution runs thus enabling its effects on the atmosphere to be resolved. The amount of irrigation given to the vegetation amounts 10 mm per day and this figure is based on irrigation projects in other parts of Saudi Arabia (Abderrahman, 2001). The initial soil moisture levels are also adjusted to account for a more realistic soil profile given the irrigation rate of 10 mm per day.

The simulations presented in this paper have been executed on the powerful supercomputer called the Earth Simulator, located at JAMSTEC in Yokohama, Japan (http://www.es.jamstec.go.jp) which can reach a theoretical peak performance of 40960 GFlops. The Earth Simulator provides a perfect scope to resolve complex terrain on a high resolution grid. To port RAMS to this supercomputer a couple of machine related changes had to be made to the original RAMS code. RAMS was set up using a message passing interface provided by the Earth Simulator Centre to execute RAMS in parallel mode. We used RAMS on in total 80 processors divided over 10 nodes. For this particular code and model configuration, using 80 processors led to a parallel efficiency of 60% while using 16 processors gave an efficiency of around

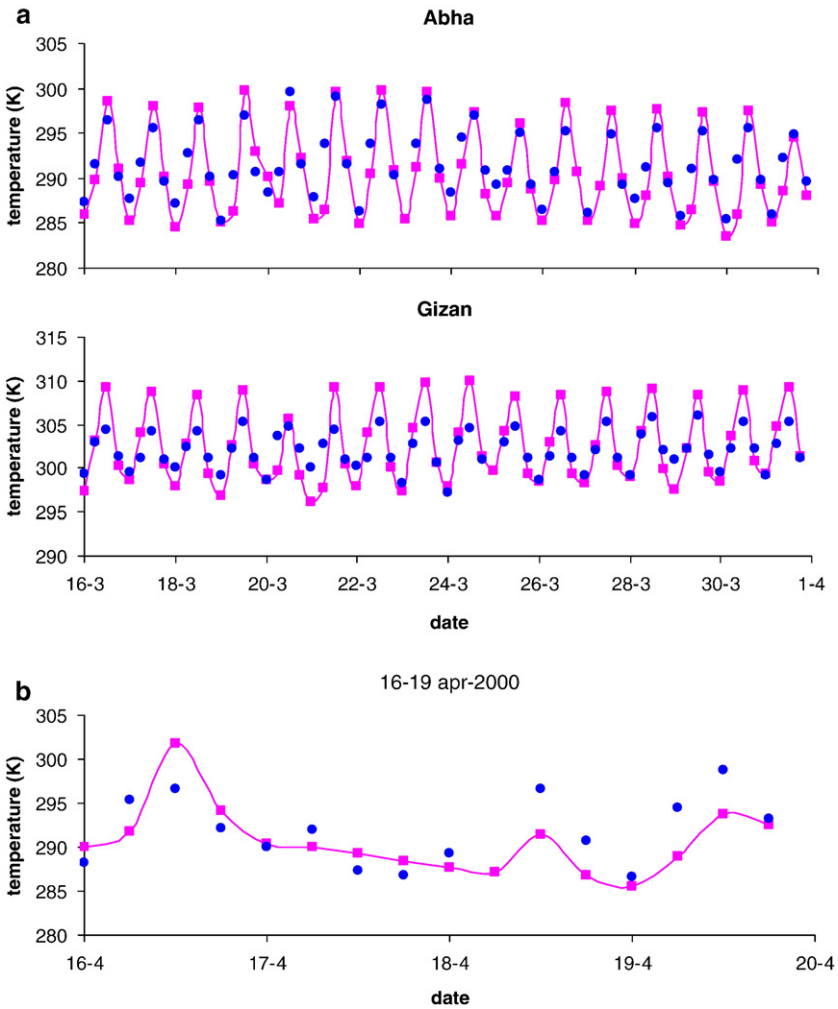

Fig. 3. a) Time series of temperature for two sites from 16 March to 31 March. b) Time series of temperature (K) at Abha from 16 April 2000 until 19 April 2000. Line with squares: simulation, dots: observations.

80%. This drop in efficiency for 80 processors is for the greatest part related to communication overhead.

Besides the machine related modifications mentioned above, a couple of model settings had to be adjusted as well to improve simulated results. During the model implementation phase we tested various setting (grid size and resolution, nesting configurations, nudging strengths) before a satisfactory control simulation was produced. One important setting for numerical stability was the representation of topography in the modelling environment. From Fig. 2 one can see that the topography rises very steep from sea level to more than 2000 m in hardly 100 km. This asks for a conservative way of interpolating the raw topography fields in order to maintain a numerical stable model. The interpolation scheme used in this study uses a conventional mean which smoothes the high peaks of the Asir Mountain range. To improve shortwave radiation at the surface, which at first was too much blocked by high altitude clouds, the 2nd moment shape parameters of the gamma distribution in the microphysics (Walko et al., 1995; Meyers et al., 1997) had to be

Table 3
Simple statistical analysis for temperature (RMSE: root mean square error; bias defined as simulated-observed)

Month	Abha		Khamis Mushait		Gizan	
	RMSE	Bias	RMSE	Bias	RMSE	Bias
February	2.25	−0.26	3.06	−1.06	2.22	0.32
March	2.68	−0.71	3.40	−1.64	2.67	−0.03
April	3.68	−1.61	4.28	−2.08	4.39	−2.25
May	3.42	0.28	3.79	−0.54	3.88	−2.36
Total	3.13	−0.81	3.74	−1.55	3.52	−1.18

adjusted to narrow the distribution spectrum and let it peak at a larger diameter. This had a positive effect on the shortwave incoming radiation at the surface, which improved the simulations compared with radiation observations (NASA Remote Sensing Validation Data, http://rredc.nrel.gov/solar/new_data/Saudi_Arabia/). To our knowledge no experimental microphysics data for this region are available to quantify the microphysics model parameters more objectively.

4. Results

The simulation results will be presented and discussed in two parts: validation and impact assessment. The first part deal with the validation of the model against surface observations and satellite data and the second part will focus on the meteorological impact assessment study of the landuse change described earlier.

4.1. Validation

The control run is compared against surface observations and satellite data to assess the performance of the model to simulate the regional climate of Southwest Arabia. In the validation against surface observations, the emphasis is on the three stations mentioned in Table 2 and indicated in Fig. 2a with two stations located in the mountain range (Abha and Khamis Mushait) and the other station located at the coast (Gizan). The initial validation is based on temperature, wind speed and wind direction as these variables were available for most of the observations. Precipitation observations at the three stations were very limited and of uncertain quality and therefore we did

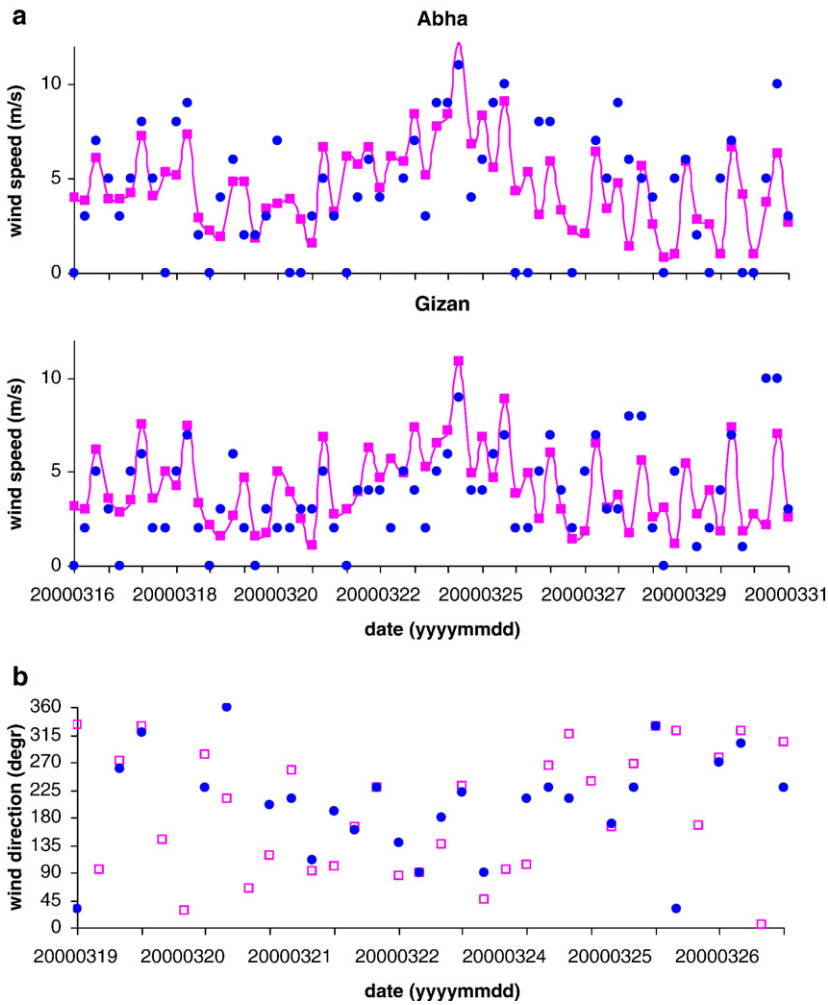

Fig. 4. a) Windspeed (m s^{-1}) simulated and observed for Abha and Gizan, from 16 March to 31 March. b) Wind direction (deg) for Gizan. squares: RAMS; dots: observations.

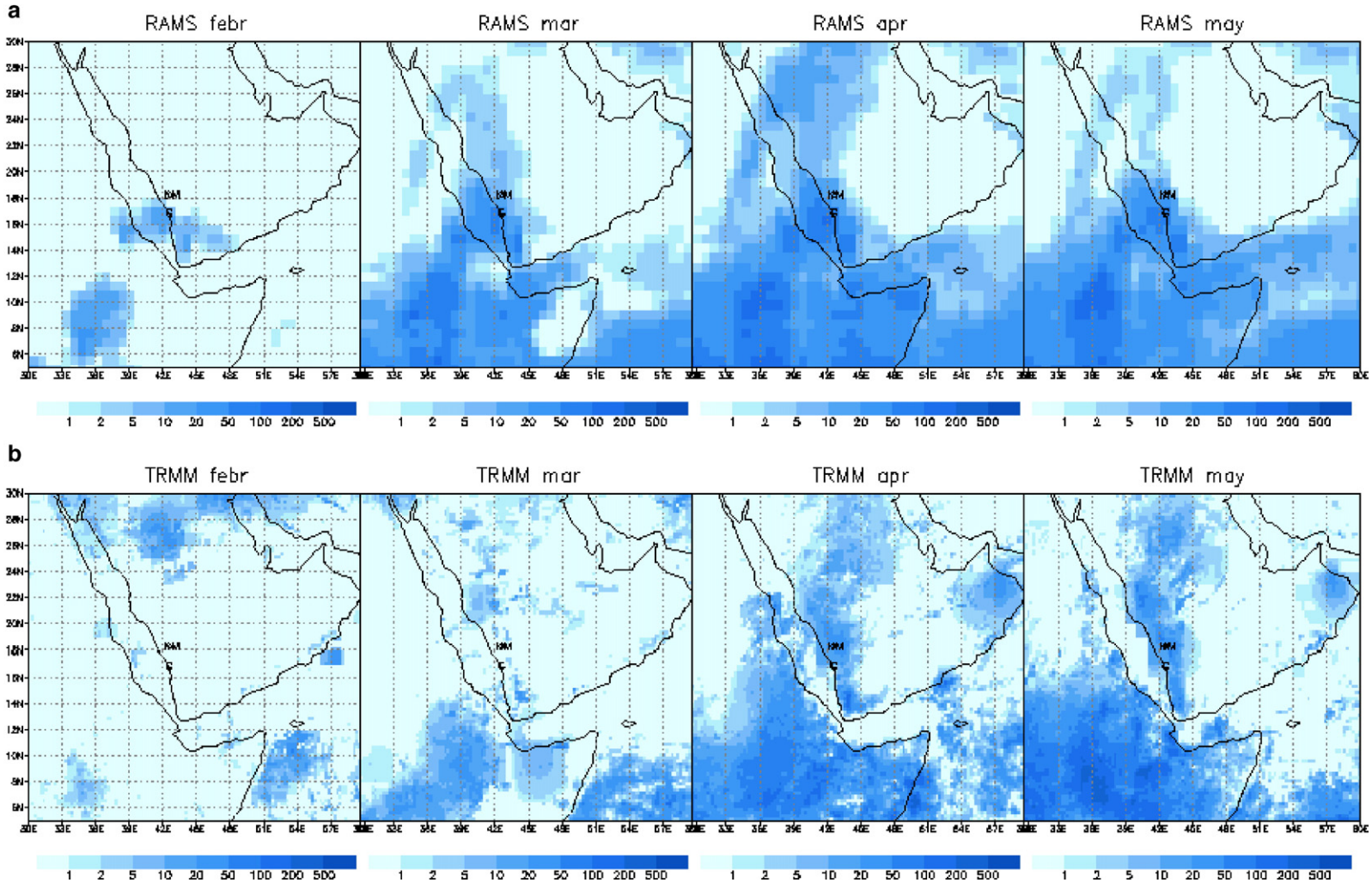

Fig. 5. Comparison between simulated and observed (TRMM 3b43 0.25° resolution) spatial patterns of monthly rainfall for the coarse resolution grid.

not validate the precipitation simulated by RAMS against these observations. As mentioned before, the simulation extends from 21 February to 15 May 2000 with output generated every six hours in phase with the synoptic times of the surface observations. To obtain stationdata out of RAMS a bilinear interpolation is performed using the four gridpoints around the coordinates of the station.

One important step, to ensure proper validation, is to bring down temperature and windspeed from the lowest model level in RAMS (48 m above ground) to surface observation level, and to adjust for altitude difference between model topography and station altitude. Similarity theory (Louis, 1979) is used to adjust model temperatures and wind speeds to the surface temperature observation level of 2 m and the surface wind observation level of 10 m. Altitude differences between station and model were used to correct simulated temperatures using the dry adiabatic lapse rate.

Fig. 3a shows the time series of temperature for the second half of March (as an example). The model is capable of simulating temperature at screen level reasonably well for this period. The agreement between model and observations is very good for Abha, however the maximum temperature is overestimated by RAMS for Gizan which may be a result of the limiting influence of the Red Sea as simulated by RAMS. During the

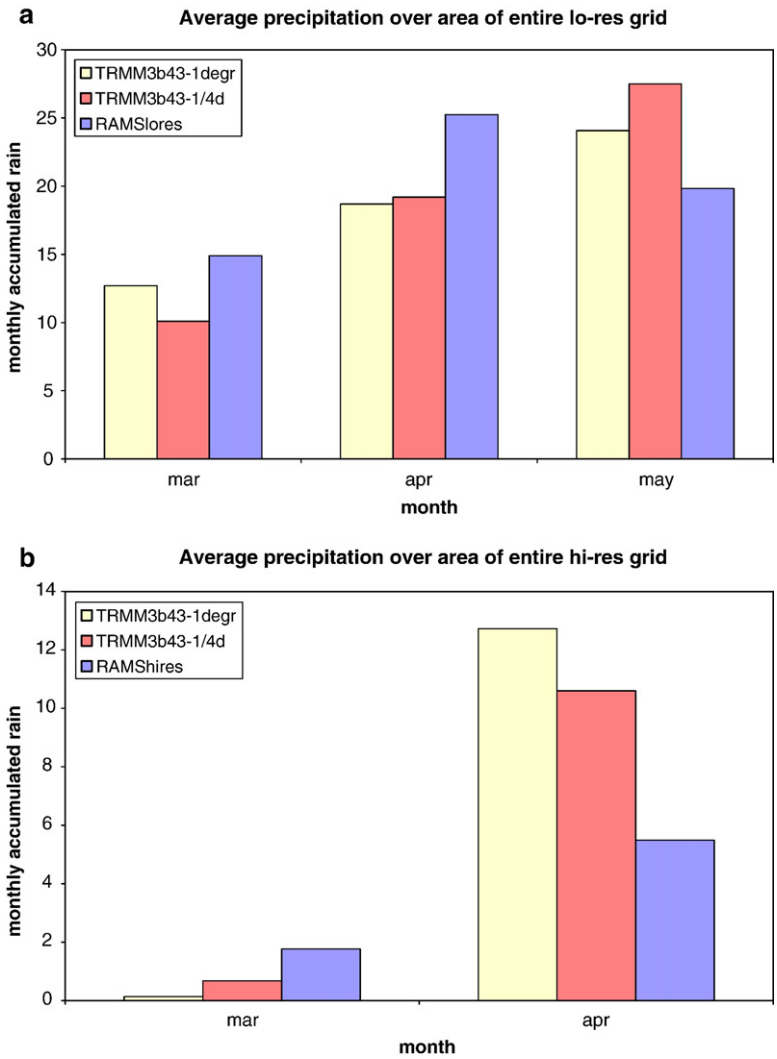

Fig. 6. Comparison between simulated (blue) and observed monthly total rainfall areally averaged for the whole domain of a) the coarse resolution grid (shown in Fig. 5), and for b) the high-resolution grid (shown in Fig. 2). Observations are based on the merged (satellite–ground observations) TRMM product 3b43 available at 2 resolution 0.25° (pink) and 1° (yellow). (For interpretation of the references to colour in this figure legend, the reader is referred to the web version of this article.)

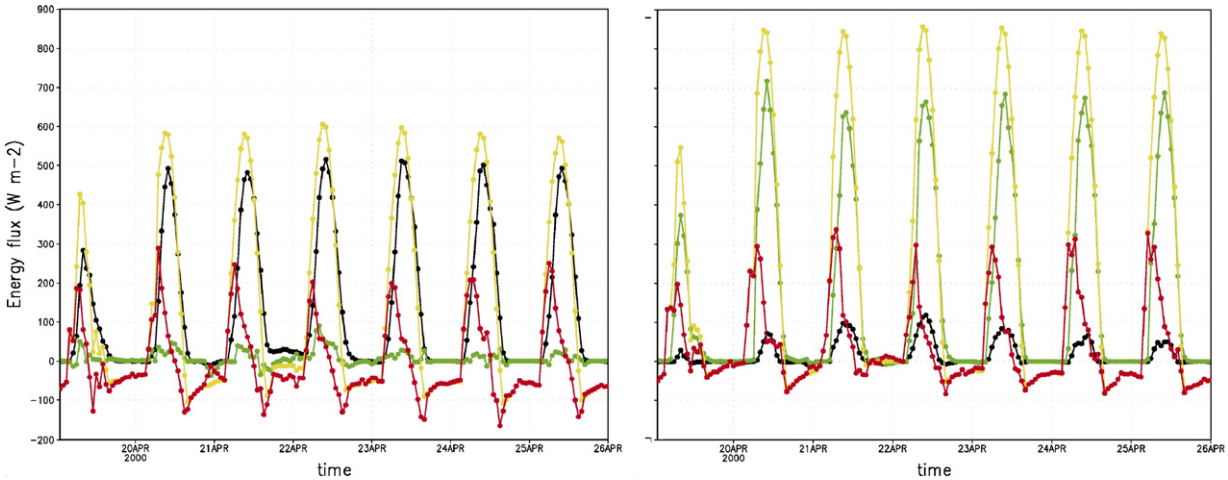

Fig. 7. Energy balances for the control run (left panel) and the green run (right panel) from 19 April to 25 April. Yellow: Net radiation (W m^{-2}), green: latent heat flux (W m^{-2}), black: sensible heat flux (W m^{-2}), red: soil heat flux (W m^{-2}). (For interpretation of the references to colour in this figure legend, the reader is referred to the web version of this article.)

simulation some events occur with a diurnal range of only a couple of degrees. This limited diurnal range is simulated by the model for all three stations, but the absolute temperature is underestimated by the model for Gizan. However, the mountain stations show a simulated temperature which is close to the observations as can be

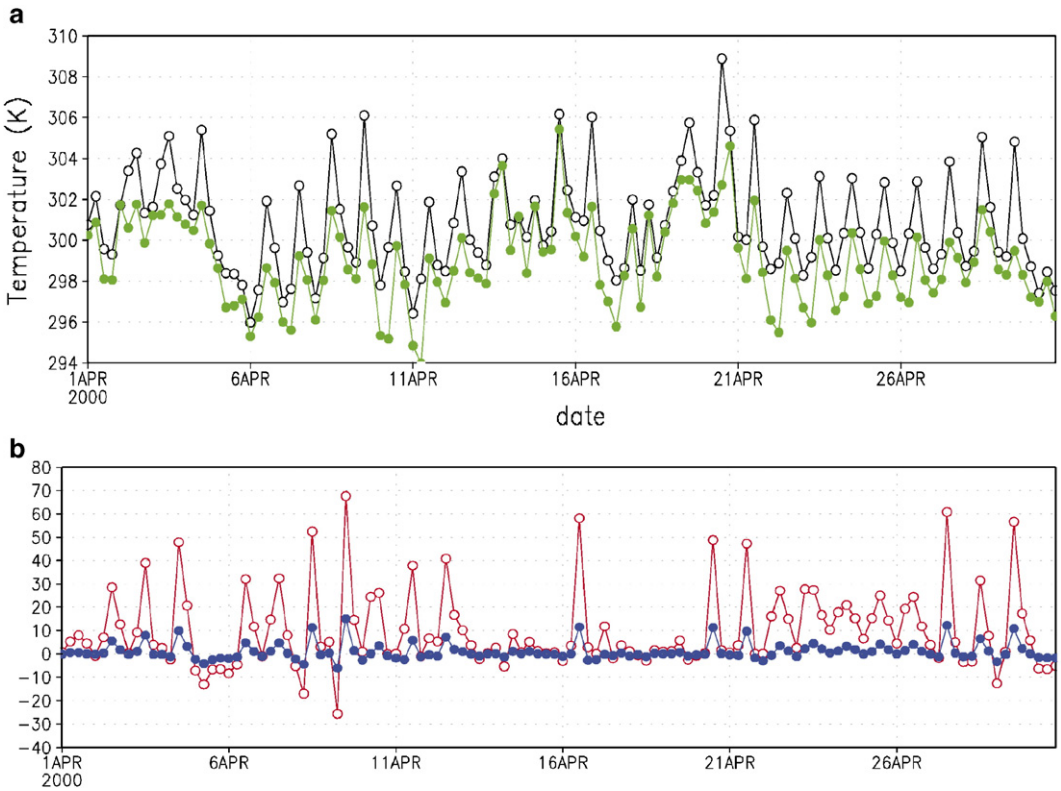

Fig. 8. a) Simulated temperature (K; black line control run, green line 'green' run) and b) difference in relative humidity (%; red line and vapor mixing ratio (g kg^{-1}, blue line) in April at the centre of the irrigated plantation. (For interpretation of the references to colour in this figure legend, the reader is referred to the web version of this article.)

seen from Fig. 3b which shows the simulated temperature and the observed temperature for a period with a small diurnal range.

Statistics of the temperature validation are given in Table 3. This table shows the monthly root mean square error (RMSE) and the bias for all three stations. The bias shows that the model in general underestimates temperature with only an overprediction for May in Abha and February in Gizan. For all three stations the RMSE peaks in April and is lowest in the first weeks of the simulation.

Fig. 4a shows an example of the evolution of wind speed for Abha and Gizan. From both graphs it can be seen that, in a qualitative way, the wind speed is simulated reasonably well by the model capturing the relative high wind speeds between 21 and 26 March. In general the model underestimates most mid-day peaks in the wind speed, and seems to overestimate night time wind speed and this applies to the whole simulation. This is more pronounced for Gizan and less for the mountain stations. Note that the values of wind speed extracted from the ECMWF archive are only archived as whole numbers.

One important local weather phenomenon in the area of interest is the occurrence of sea breeze events as observable in the record of the coastal station of Gizan. Fig. 4b shows the development of sea breezes in both observations and model output. In the course of a day the wind changes from an easterly wind to a southwesterly wind. Fig. 4b also shows the probable influence of more synoptically driven wind from 24 March onward, obstructing the development of a sea breeze, which is partly simulated by RAMS.

Since only a few ground stations exist in our domain, the most important source for validation of magnitude and areal distribution of precipitation is the TRMM rainfall product 3B43. Fig. 5 compares simulated and observed spatial patterns of monthly rainfall for the larger grid. It shows that in general patterns of precipitation are simulated well, though our model simulation gives more wide-spread rain over the Red Sea and Indian Ocean, especially in April and May. This is confirmed in Fig. 6a which gives monthly rainfall areally averaged over entire domain of the coarse resolution grid (the extend is shown in Fig. 5). It shows the average numbers do not differ significantly between model and observation. Fig. 6b shows the same for the high resolution grid for the two full months that fall in the simulated period (21 February–15 May). It shows that the high resolution simulation seems to underestimate total rainfall in April, and it also simulates rain more localized than in reality. In March the opposite is true. Note the small absolute values of rain in both Fig. 6a and b. It further shows that the TRMM rainfall product gives different totals depending on the resolution of the 3b43 product. Since this latter

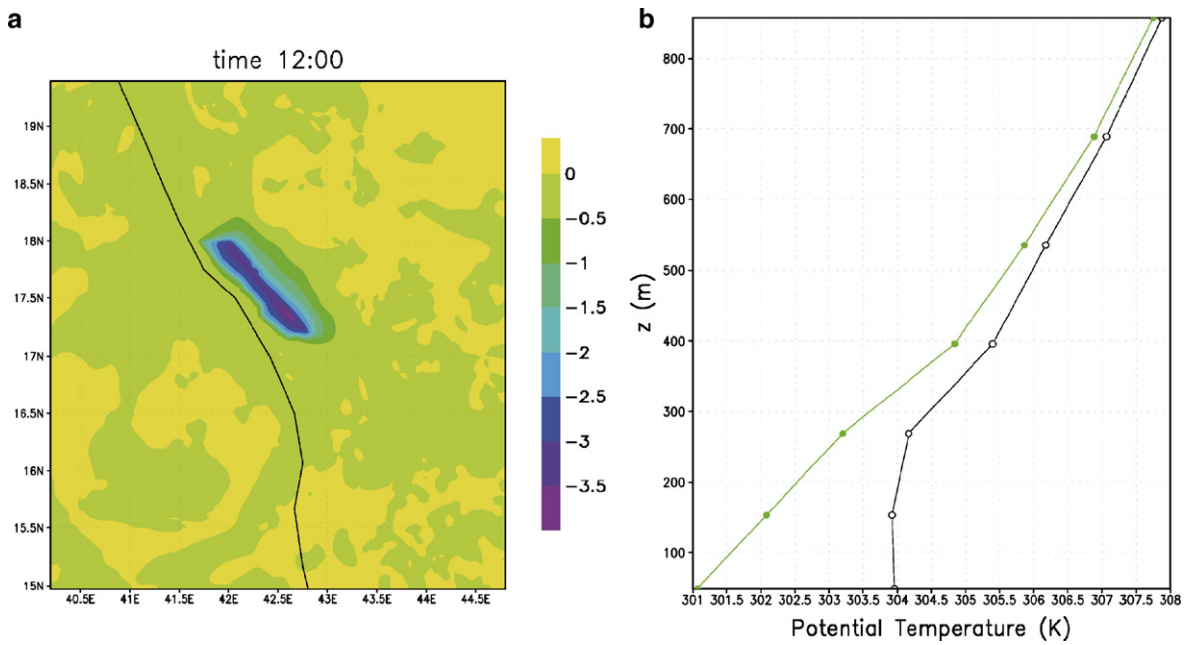

Fig. 9. a) Spatial representation of the difference in temperature at 12:00 UTC averaged for April. The difference is calculated as green-control. b) Vertical profile of the potential temperature (K) at 12:00 UTC averaged for April at the reference point in the irrigation plantation. Black — control run; green — 'green' run. (For interpretation of the references to colour in this figure legend, the reader is referred to the web version of this article.)

phenomenon is more pronounced for individual grid-boxes and the localized nature of actual and simulated rainfall we do not show a validation at station level as it is very inconclusive.

4.2. Impact assessment

This section will deal with the difference between the control run and the green run, which is defined as the

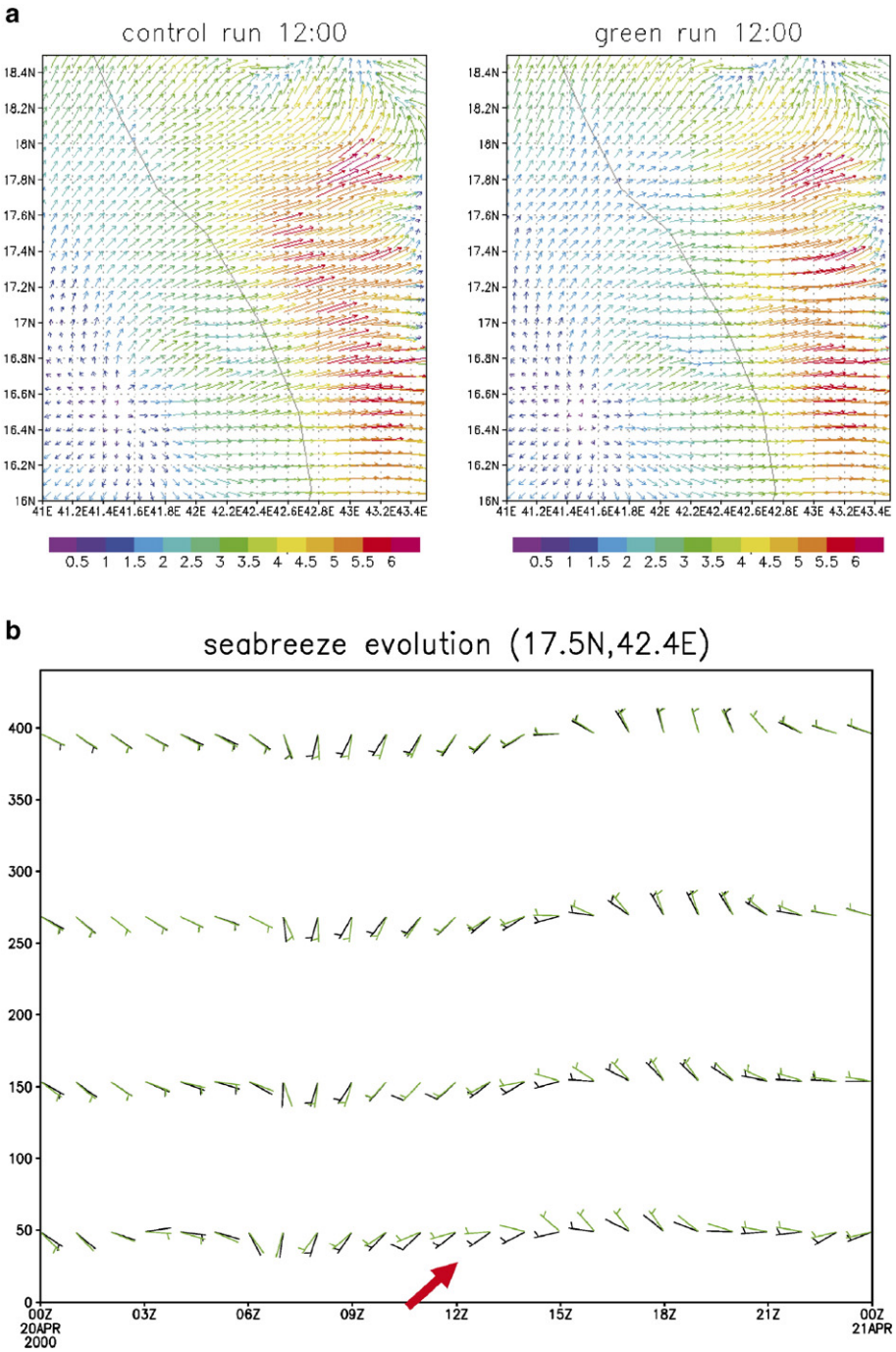

Fig. 10. a) Spatial representation of wind vectors for the control simulation (left panel) and the green simulation (right panel) at 12:00 UTC (average for April). The color of the vectors represents the simulated wind speed in m s^{-1}. b) Vertical daily profile of the wind vectors simulated at centre of the plantation (17.5°N, 42.4°E) for 20 April 2000. Black — control run; green — 'green' run. The red arrow gives the direction orthogonal to the coast line at this latitude. (For interpretation of the references to colour in this figure legend, the reader is referred to the web version of this article.)

simulation where an irrigated plantation has been implemented in the model (see Fig. 2a for the precise location of this plantation). Both simulations use the same meteorological boundary and initial conditions. Various analyses have been done to assess the differences but most of the analysis presented here focuses on the month of April 2000.

We start the impact assessment with the simulated effect of the irrigated plantation on the energy balance and the partitioning of energy over the various heat fluxes. Fig. 7 shows the four important variables in the energy balance for the control simulation and the green simulation. The figure shows the balance for a week at the end of April with an hourly resolution. The biggest difference between both graphs is the change in latent heat flux which is for most of the days between 600 and 700 W m^{-2}, resulting in a change of evaporative fraction from 0.05 to about 0.9. The evaporative fraction (unitless) is defined as $\lambda = LE/(H+LE)$, with LE latent heat flux (W m^{-2}) and H sensible heat flux (W m^{-2}). The irrigation rate of 10 mm per day results in a high transpiration as a result of high incoming radiation and low relative humidity, to. Another effect in the energy balance is the change of net radiation, which is raised in the green simulation by 25%. This increase is a direct result of a change in albedo accompanied with the change in vegetation from desert to the irrigated plantation.

Fig. 8a shows two time series of temperature (°C) for April simulated for a location in the middle of the plantation (42.4°N and 17.5°E) that will be used in other graphs presented here as well. The simulated temperature is lower in the green run, which is a result of the cooling effect induced by the vegetation. The vegetation absorbs energy which is transformed into latent energy by plant transpiration, which leads to lower temperatures at the surface level. This cooling effect appeared to be higher on those days where the simulated vapor mixing ratio was relatively high, most possibly triggering a higher rate of transpiration of the vegetation. The difference between the control and green simulation is most noticeable greater during midday but is even apparent at nighttime when the difference between both simulations is on average around 1 °C. The cooling effect is mostly limited to the irrigation plantation (Fig. 9a) with a maximum cooling effect of 3.5 °C at 12:00 UTC. During daytime a small area downwind (i.e. inland) of the plantation also appeared to experience a small cooling effect. Model soundings show that the cooling effect of the plantation propagates upward until 700 m above ground level at daytime (Fig. 9b) and 200 m at nighttime (not shown).

Because of the transpiring vegetation, the humidity in the surrounding of the irrigated plantation is affected as well. Fig. 8b shows the increase in relative humidity

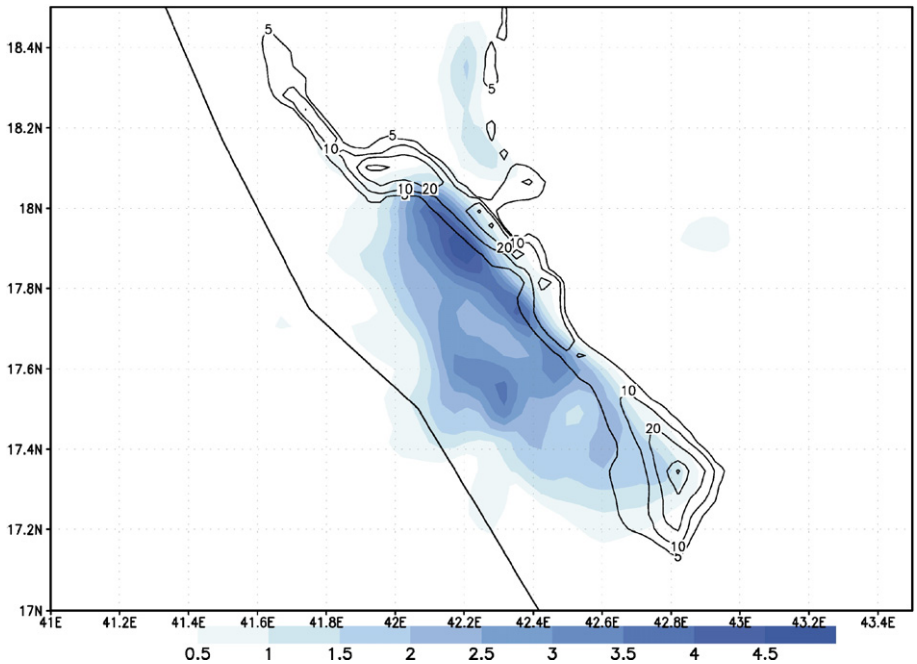

Fig. 11. Spatial distribution of the difference in precipitation (mm) between green and control run for the whole February to May simulation. The thin black contours shows the relative increase (–), defined as (green-control)/control of precipitation (contour levels are at 5, 10, 20, 40 and 60%). (For interpretation of the references to colour in this figure legend, the reader is referred to the web version of this article.)

between the green and control simulations. Vapor mixing ratio is increased by a few g kg^{-1}, occasionally up to more than 10 g kg^{-1}. Due to simultaneous cooling the effect on relative humidity is more pronounced. The increase is more profound in February and March (increase in relative humidity by >15% on average) than in April and May (~10% relative humidity increase).

In direct relation with the temperature change in the irrigated plantation changes in wind speed and wind direction occur. The strength of the sea breeze depends on the difference in temperature between the Red Sea and the land surface. The cooling effect in the green simulation therefore leads to a decrease in the strength of the sea breeze which is nicely simulated by the model (Fig. 10a).

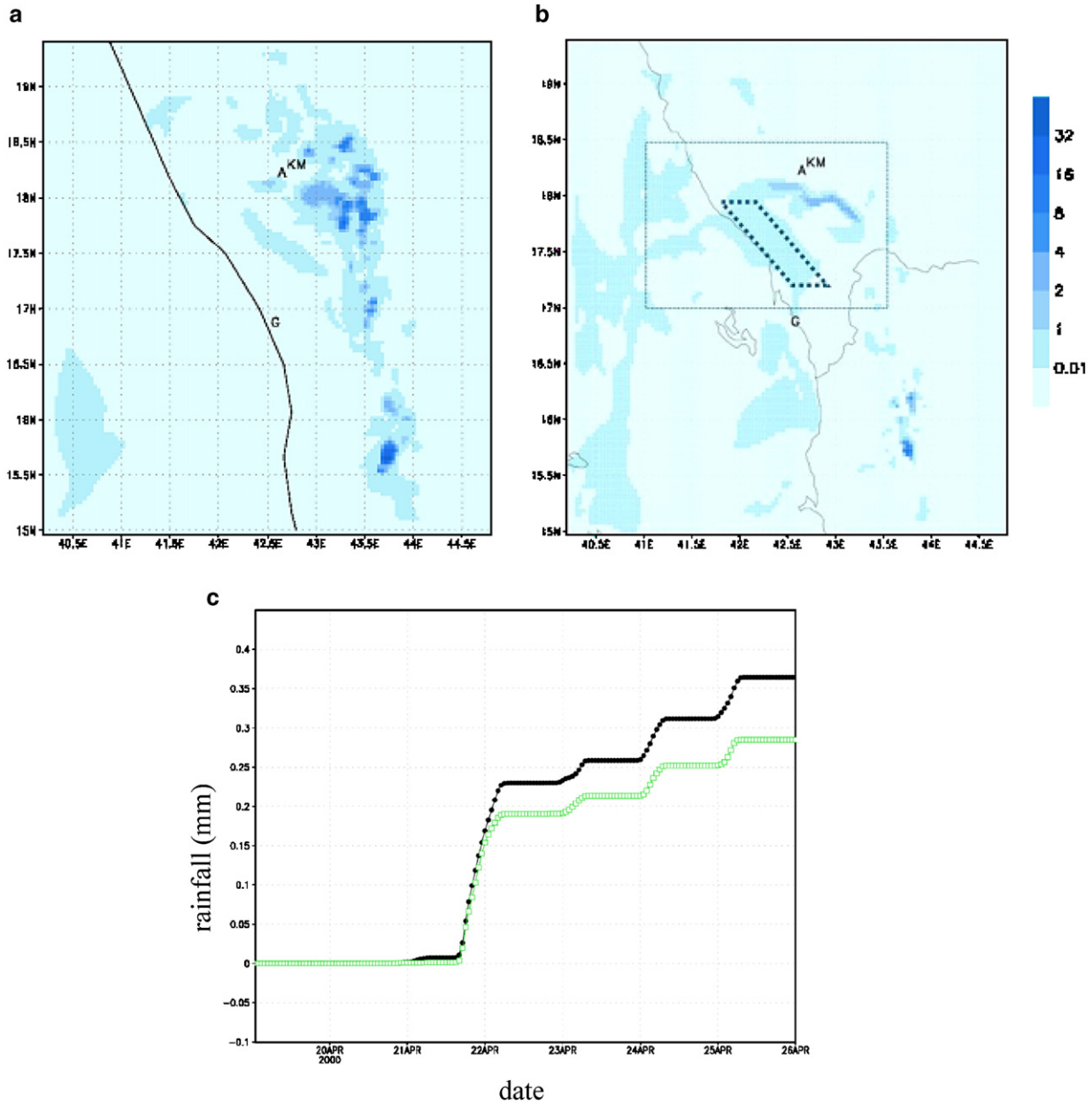

Fig. 12. Case study of 1 week simulation for 19–26 April 2002. a) Total rainfall (mm) for same period for control run. b) Total rainfall difference (mm) for 'green' vs. control runs. The skewed rectangle depicts the area of the irrigated plantation. The square outlines the area for which Fig. 12c applies and for which numbers are given in the text. c) Areal average rain (mm) for control (black filled circles) and green (green open circles) runs. (For interpretation of the references to colour in this figure legend, the reader is referred to the web version of this article.)

The velocity of the sea breeze is about one third smaller in the green simulation compared to the control simulation. Not only the velocity is affected by the change in vegetation but also the wind direction is shifted to a more (north) westerly flow compared to the southwest winds which are more perpendicular to the Arabian coastline. Fig. 10b shows this clearly in a vertical profile for a certain day (20 April in this example) and at a higher time resolution (hourly) for the centre of the plantation.

Most interesting in this analysis is to see the impact of the vegetation change and change in soil moisture on precipitation. We analyse two effects: a local effect and a downwind effect. Fig. 11 shows the local effect: the difference in precipitation between both simulations for an area directly over and around the irrigated plantation. The precipitation increase resulting from the irrigation plantation is apparent and is most visible over and just downwind of the plantation and concentrates at the northern part of the plantation. The increase is small in absolute numbers (averaged over the affected area from 1.5 to 3.7 mm) but large in relative numbers. This local increase in precipitation is more pronounced in February and March, weakens in April and is almost zero in May.

For the downwind effect, we next present an analysis for one particular week in April. Started from history files we saved model output at higher temporal resolution. For this particular run Fig. 12a shows that precipitation was well simulated: Khamis (KM in the figure) rainfall in this week was 31.7 mm and for Gizan 0 mm. Fig. 12b shows the effect of the irrigated plantation which increases precipitation on the windward side of first mountain ridges (compare Fig. 2). As the time series in Fig. 12c show total rainfall (averaged over the square in 12b) increased by 34%. It also shows that most rainfall occurs at night. Detailed analyses using animation of the time series showed that the following process is responsible. During daytime a significant 'blob' of wet air develops over the irrigated plantation. With the onset of the sea-breeze this start being transported by the wind in easterly direction, uphill to the Asir Mountain range, where in the early evening fog starts to develop. Later at night then, light rains develop which stop as soon as the sun rises. The same mechanism occurs in the control run with moist air from the Red sea being blown by the sea breeze onto the mountains. Apparently, the extra moisture in the 'blob' originating from the plantation leads to the extra rain.

5. Discussion

We will discuss the validation and impact assessment parts separately.

5.1. Validation of control run

Our simulations seem to overestimate the diurnal range in temperature, especially for the coastal station of Gizan. One reason may be that in daytime our model overestimates sensible heat fluxes and underestimates latent heat flux. The only data on energy partitioning available to date have been measured at the old airport near Jeddah for most of 2004 (R. Ohba, personal communication). Though obtained outside our domain these data suggest (see Fig. 7) that simulated net radiation is reasonable but that the simulated Bowen ratio is too high (~10 simulated vs. ~4–5 observed). This may be related to the fact that in our model setup the 'desert' land use class has no vegetation at all, which may not be realistic. Night time sensible heat fluxes are remarkably small in both observations and model.

Wind speed and direction are well simulated, especially the occurrence of sea breeze phenomena. We consider this important because the hypothesized role sea breezes may play in advecting moist marine air to land.

Validation of precipitation in this particular area is complicated by a number of factors. As in semi-arid areas in general, any rain that occurs is highly intermittent and localized. The number of ground stations is limited (3 in our domain) and the quality of the observations is questionable. Also TRMM estimates differ with resolution. Therefore, a validation at local (station level) scales remains inconclusive. At larger scales validation is possible and it seems to reveal that RAMS in this particular setting over-estimates rainfall at coarse resolutions, that is, when using the convective parameterization. On the other hand RAMS seems to underestimate rainfall at higher, cloud resolving resolutions using its microphysics parameterization. Also model performance seems to differ between long and short runs. We realize that these deficiencies do limit the robustness of the conclusions drawn later.

5.2. Impact of irrigated plantation

The effects of increased vegetation density and daily soil moisture repletion, as introduced by our hypothetical irrigated plantation, on the energy balance and partitioning are the expected ones. As a result the air passing over the 'oasis' is cooled (by 3–4 K) and moistened (relative humidity increased by 10 to 15%).

The wind climate of the coastal area of SW Saudi Arabia is amongst others characterised by daily occurrence of sea breezes. Since the irrigated plantation in that area decreases the thermal contrast between land and sea, the sea breeze weakens both in magnitude and directional

change. This effect of coastal land cover changes in general (Pielke at al. 1999; Baker et al., 2001; van der Molen, 2002; Marshall et al., 2004) and coastal irrigation in particular has been reported by others (Lohar and Pal, 1995). It may be one of the reasons of the limited effect on rainfall. On the one hand because it limits the transport of the extra moisture land inward. On the other hand because it reduces the chance that the sea breeze triggers convective phenomena that may be more effective in rainfall generation, as discussed next.

Though we need to be cautious with respect to our conclusions on the effects of our hypothetical irrigated plantation on rainfall is seems justified to conclude that in a setting like the one discussed here rainfall increases are limited in absolute magnitude. Though our case study for late April suggested that the increase can be up to 34% in some periods, the overall effect is small. The reason for this is that in our simulations no extra triggering of convection occurs, as is the main cause for precipitation increases in other studies (De Ridder and Gallèe, 1998; Moore and Rojstaczer, 2002). The total area of our irrigated plantation probably plays some role. Total area of our oasis is $0.32.10^8$ m^2 as compared to e.g. about $1.5.10^8$ m^2 in De Ridder and Gallèe (1998) for a case in SW Israel or more than 6.10^8 m^2 for a case in the US (Texas High plains) in Moore and Rojstaczer (2002). Also the analysis in Pielke (2001) suggest that landscape variations have their largest influence on generating local wind circulations, which may act as triggers for deep convection, for horizontal spatial scales of the order of the Rossby radius which has a typical value of $\sim 10^5$ m. However, we have to realize that these studies hypothesize a minimum area in order to generate local circulations, whereas in our case it is rather vice versa. Here a local circulation (sea breeze) is present which is weakened in response to the land cover change, and an increased irrigated area will rather suppress than enhance this circulation. The rainfall increase we do observe seems to originate in the extra moisture added to the air and not in triggering potentially larger atmospheric reservoirs. But since the sea breeze is weakened this moist air is only partially advected inland i.e. uphill to condensation levels.

6. Conclusions

The limited effects of the irrigated plantation on rainfall generation, in the particular setting reported here, seem to be caused by added moisture in an otherwise only little affected mesoscale flow. The reason for this is probably the limited size of the hypothetical oasis in the direction perpendicular to the main flow.

Finally some comments on the possibility of recycling of irrigation water, through evapotranspiration and subsequent rainfall enhancement. When we analyse the case study for the last week of April (Fig. 12c) and compute numbers for the square area delineated in Fig. 12b the following picture emerges. The total prescribed irrigation gift in that period was $193 \cdot 10^6$ m^3. This led to an increase of evapotranspiration of $115 \cdot 10^6$ m^3. The extra atmospheric moisture resulting from this increased rainfall by $2.3 \cdot 10^6$ m^3. This occurred downwind but still on the same side of the water divide in the mountains, theoretically (but by no means practically) allowing capture of this rain and feeding it back to the irrigated area. Two conclusions can be drawn from these numbers. The first is that irrigation of 10 mm per day is too much. Potentially transpiring shrub vegetation in our simulation uses about 5–6 mm per day. Secondly, recycling of this water is limited to just 2%. On one hand this is additional rain is too limited and too dispersed to re-capture and return to the irrigated area itself. On the other hand it falls in an area where rain fed agriculture occurs. There, though small in absolute numbers but big in relative numbers ($\sim$30%), the extra rain may increase crop productivity or reduce the risk of crop failures and thus be important to local agriculture (Otterman et al., 1990).

To strengthen such conclusions better statistics on more rainfall events are needed. We therefore are currently extending our simulations to cover at least a full year and have plans to repeat these for climatologically more wet or more dry years.

Acknowledgements

This study is supported by the Revolutionary Research Project (RR2002) of Ministry of Education, Culture, Sports, Science and Technology in JAPAN through Mitsubishi Heavy Industries Ltd. We are thankful to Dr. Behera, Dr. Adachi and Mr. Hara for their support in carrying out this research. The discussions and suggestions provided by Dr. Craig Tremback are greatly acknowledged.

References

Abderrahman, W.A., 2001. Energy and water in arid developing countries: Saudi Arabia, a case-study. International Journal of Water Resources Development 17 (2), 247–255.

Avissar, R., Schmidt, T., 1998. An evaluation of the scale at which ground-surface heat flux patchiness affects the convective boundary layer using large-eddy simulations. Journal of the Atmospheric Sciences 55 (16), 2666–2689.

Baker, R.D., Lynn, B.H., Boone, A., Tao, W.-K., Simpson, J., 2001. The influence of soil moisture, coastline curvature, and land-breeze circulations on sea-breeze initiated precipitation. Journal of Hydrometeorology 2, 193–211.

Bazuhair, A.S., AlGohani, A., Sen, Z., 1997. Determination of monthly wet and dry periods in Saudi Arabia. International Journal of Climatology 17 (3), 303–311.

Ben-Gai, T., Bitan, A., Manes, A., Alpert, P., 1993. Long term October rainfall patterns in S Israel. Theoretical and Applied Climatology 46, 209–217.

Chakraborty, A., Behera, S.K., Mujumdar, M., Ohba, R., Yamagata, T., 2006. Diagnosis of tropospheric moisture over Saudi Arabia and influences of IOD and ENSO. Monthly Weather Review 134 (2), 598–617.

Charney, J.G., 1975. Dynamics of deserts and drought in Sahel. Quarterly Journal of the Royal Meteorological Society 101 (428), 193–202.

Chen, C., Cotton, W.R., 1983. A one-dimensional simulation of the stratocumulus-capped mixed layer. Boundary Layer Meteorology 25, 289–321.

Claussen, M., Kubatzki, C., Brovkin, V., Ganopolski, A., Hoelzmann, P., Pachur, H.J., 1999. Simulation of an abrupt change in Saharan vegetation in the mid-Holocene. Geophysical Research Letters 26 (14), 2037–2040.

Claussen, M., Brovkin, V., Ganopolski, A., Kubatzki, C., Petoukhov, V., 2003. Climate change in northern Africa: the past is not the future. Climatic Change 57 (1–2), 99–118.

Cotton, W.R., Pielke, R.A., Walko, R.L., Liston, G.E., Tremback, C.J., Jiang, H., McAnelly, R.L., Harrington, J.Y., Nicholls, M.E., Carrio, G.G., McFadden, J.P., 2003. RAMS 2001: current status and future directions. Meteorology and Atmospheric Physics 82 (1–4), 5–29.

De Ridder, K., Gallèe, H., 1998. Land surface-induced regional climate change in southern Israel. Journal of Applied Meteorology 37, 1470–1485.

Dickinson, R.E., Henderson-Sellers, A., Kennedy, P.J., Wilson, M.F., 1986. Biosphere–Atmosphere Transfer Scheme for the NCAR Community Climate Model. NCAR Tech. Rep. NCAR/TN 2751STR. 69 pp.

Flatau, P.J., Tripoli, G.J., Verlinde, J., Cotton, W.R., 1989. The CSU-RAMS cloud microphysical module: General theory and code documentation. 451, Colorado State Univ., Fort Collins, Colorado.

Global Soil Data Task Group. 2000. Global Gridded Surfaces of Selected Soil Characteristics (IGBP-DIS). [Global Gridded Surfaces of Selected Soil Characteristics (International Geosphere-Biosphere Programme - Data and Information System)]. Data set. Available on-line [http://www.daac.ornl.gov] from Oak Ridge National Laboratory Distributed Active Archive Center, Oak Ridge, Tennessee, U.S.A.

Huffman, G.J., Adler, R.F., Rudolf, B., Schneider, U., Keehn, P.R., 1995. Global precipitation estimates based on a technique for combining satellite-based estimates, rain-gauge analysis, and Nwp model precipitation information. Journal of Climate 8 (5), 1284–1295.

Kabat, P., Claussen, M., Gash, J.H.C., Dirmeyer, P., Meybeck, M., Vörösmarty, C.J., Pielke, R.A., Hutjes, R.W.A., Lutkemeier, S. (Eds.), 2004. Vegetation, Water, Humans and the Climate: a New Perspective on an Interactive System. Springer Verlag.

Koster, R.D., Dirmeyer, P.A., Guo, Z.C., Bonan, G., Chan, E., Cox, P., Gordon, C.T., Kanae, S., Kowalczyk, E., Lawrence, D., Liu, P., Lu, C.H., Malyshev, S., McAvaney, B., Mitchell, K., Mocko, D., Oki, T., Oleson, K., Pitman, A., Sud, Y.C., Taylor, C.M., Verseghy, D., Vasic, R., Xue, Y.K., Yamada, T., 2004. Regions of strong coupling between soil moisture and precipitation. Science 305 (5687), 1138–1140.

Lohar, D., Pal, B., 1995. The effect of irrigation on premonsoon season precipitation over south-west Bengal, India. Journal of Climate 8 (10), 2567–2570.

Louis, J.F., 1979. Parametric model of vertical eddy fluxes in the atmosphere. Boundary - Layer Meteorology 17 (2), 187–202.

Loveland, T.R., Reed, B.C., Brown, J.F., Ohlen, D.O., Zhu, Z., Yang, L., Merchant, J.W., 2000. Development of a global land cover characteristics database and IGBP DISCover from 1 km AVHRR data. International Journal of Remote Sensing 21 (6–7), 1303–1330.

Marshall, C.H., Pielke, R.A., Steyaert, L.T., Willard, D.A., 2004. The impact of anthropogenic land-cover change on the Florida peninsula sea breezes and warm season sensible weather. Monthly Weather Review 132 (1), 28–52.

Mellor, G.L., Yamada, T., 1982. Development of a turbulence closure model for geophysical fluid problems. Reviews of Geophysical and Space Physics 20 (4), 851–875.

Meyers, M.P., Walko, R.L., Harrington, J.Y., Cotton, W.R., 1997. New RAMS cloud microphysics parameterization. Part II: the two-moment scheme. Atmospheric Research 45 (1), 3–39.

Moore, N., Rojstaczer, S., 2002. Irrigation's influence on precipitation: Texas High Plains, USA. Geophysical Research Letters 29 (16).

Otterman, J., Manes, A., Rubin, S., Alpert, P., Starr, D., 1990. An increase of early rains in southern Israel following land use change? Boundary - Layer Meteorology 53, 333–351.

Pielke, R.A., 2001. Influence of the spatial distribution of vegetation and soils on the prediction of cumulus convective rainfall. Reviews Of Geophysics 39 (2), 151–177.

Pielke, R.A., Walko, R.L., Steyaert, L.T., Vidale, P.L., Liston, G.E., Lyons, W.A., Chase, T.N., 1999. The influence of anthropogenic landscape changes on weather in south Florida. Monthly Weather Review 127, 1663–1673.

Pielke, R.A., Marland, G., Betts, R.A., Chase, T.N., Eastman, J.L., Niles, J.O., Niyogi, D., Running, S., 2002. The influence of land-use change and landscape dynamics on the climate system: relevance to climate-change policy beyond the radiative effect of greenhouse gases. Philosophical Transactions of the Royal Society of London. Series A Mathematical, Physical and Engineering Sciences 360 (1797), 1705–1719.

Rayner, N.A., Parker, D.E., Horton, E.B., Folland, C.K., Alexander, L. V., Rowell, D.P., Kent, E.C., Kaplan, A., 2003. Global analyses of sea surface temperature, sea ice, and night marine air temperature since the late nineteenth century. Journal of Geophysical Research-Atmospheres 108 (D14).

Reynolds, J.F., Stafford-Smith, D.M., 2002. Global desertification, do humans cause deserts? Dahlem Workshop Report, vol. 88. Dahlem Univ Press, Berlin.

Schickedanz, P.T., Ackermann, W.C., 1977. Influence of irrigation on precipitation in semi-arid climates. In: Worthington, E.B. (Ed.), Arid Land Irrigation in Developing Countries. Pergamon Press, pp. 185–196.

Sud, Y.C., Mocko, D.M., Walker, G.K., Kosgter, R.D., 2001. Influence of land surface fluxes on precipitation: inferences from simulations forced with four ARM-CART SCM datasets. Journal Of Climate 14 (17), 3666–3691.

Tremback, C.J., 1990. Numerical simulation of a mesoscale convective complex: model development and numerical results. PhD Diss., Atmos Sci Paper No 465, Colorado State University, Department of Atmospheric Science, Fort Collins, CO 80523.

van der Molen, M.K., 2002. Meteorological impacts of land use change in the maritime tropics. Ph. D. Thesis. Vrije Universiteit, Amsterdam, The Netherlands.

Walko, R.L., Cotton, W.R., Meyers, M.P., Harrington, J.Y., 1995. New RAMS cloud microphysics parameterization. Part I: the single-moment scheme. Atmospheric Research 38 (1), 29–62.

Walko, R.L., Band, L.E., Baron, J., Kittel, T.G.F., Lammers, R., Lee, T.J., Ojima, D., Pielke, R.A., Taylor, C., Tague, C., Tremback, C.J., Vidale, P.L., 2000. Coupled atmosphere-biophysics-hydrology models for environmental modeling. Journal of Applied Meteorology 39 (6), 931–944.

Xue, Y., Hutjes, R.W.A., Harding, R.J., Claussen, M., Prince, S., Lambin, E.F., Alan, S.J., Dirmeyer, P., 2004. The Sahelian climate. In: Kabat, P., et al. (Eds.), Vegetation, Water, Humans and the Climate: a New Perspective on an Interactive System. Springer Verlag.